Nat Hazards (2018) 90:693–704
https://doi.org/10.1007/s11069-017-3062-5

ORIGINAL PAPER

Prediction of spatial soil organic carbon distribution using Sentinel-2A and field inventory data in Sariska Tiger Reserve

Pavan Kumar[1] · Haroon Sajjad[1] · Bismay Ranjan Tripathy[2] · Raihan Ahmed[1] · Vinay Prasad Mandal[1]

Received: 16 August 2017 / Accepted: 12 October 2017 / Published online: 24 October 2017

Abstract Dynamic and vigorous top soil is the source for healthy flora, fauna, and humans, and soil organic matters are the underpinning for healthy and productive soils. Organic components in the soil play significant role in stimulating soil productivity processes and vegetation development. This article deals with the scientific demand for estimating soil organic carbon (SOC) in forest using geospatial techniques. We assessed distribution of SOC using field and satellite data in Sariska Tiger Reserve located in the Aravalli Hill Range, India. This study utilized the visible and near-infrared reflectance data of Sentinel-2A satellite. Three predictor variables namely Normalized Difference Vegetation Index, Soil Adjusted Vegetation Index, and Renormalized Difference Vegetation Index were derived to examine the relationship between soil and SOC and to identify the biophysical characteristic of soil. Relationship between SOC (ground and predicted) and leaf area index (LAI) measured through satellite data was examined through regression analysis. Coefficient of correlation (R^2) was found to be 0.95 (p value < 0.05) for predicted SOC and satellite measured LAI. Thus, LAI can effectively be used for extracting SOC using remote sensing data. Soil organic carbon stock map generated through Kriging model

✉ Haroon Sajjad
haroon.geog@gmail.com

Pavan Kumar
pawan2607@gmail.com

Bismay Ranjan Tripathy
bismaytripathy@outlook.com

Raihan Ahmed
raihan.geog@gmail.com

Vinay Prasad Mandal
vinnumandal@gmail.com

[1] Department of Geography, Faculty of Natural Sciences, Jamia Millia Islamia, New Delhi 110025, India

[2] Department of Remote Sensing and GIS, National Centre for Earth Science Studies Earth System Science Organization, Thiruvananthapuram, India

for Landsat 8 OLI data demonstrated variation in spatial SOC stocks distribution. The model with 89% accuracy has proved to be an effective tool for predicting spatial distribution of SOC stocks in the study area. Thus, optical remote sensing data have immense potential for predicting SOC at larger scale.

Keywords Soil organic carbon · Predictor variables · Leaf area index · Kriging spatial interpolation · RMSE

1 Introduction

Soil being a vital part of our ecosystem forms a substratum for sustaining life on the Earth. It is estimated that about 75% of total carbonic stock of terrestrial ecosystem lies in soil. The carbon content in soil is most important parameter for examining soil quality and soil health (Brown 1997). Forest Inventory and Analysis (FIA) with its baseline regional carbon assessment reports have helped researchers to understand about carbon content and harvested wood products in forest ecosystems (Gullison et al. 2007; Wu et al. 2009; Houghton et al. 2009). The information about the relationship among the carbon storage, past management, and disturbance impacts can be retrieved from the varied trends of the carbon stocks along with the companion assessments on forest carbon disturbances (Tekin et al. 2012). This associated information can be used to assess the short- and long-term carbon consequences for alternative forest strategies. The climate change and global warming have created severe negative inferences to environment all over world. Carbon dioxide alone supplies about 60% of the total worldwide warming and plays an important role in carbon sequestration. "Soil organic carbon (SOC)," which is a part of natural carbon cycle—the quantity of carbon stored in the soil—is a constituent of soil organic matter, produced by disintegration of plant and animal materials at various stages in soil (Barnes et al. 2003; Gao and Goetz 1990; McBratney et al. 2003). Soil organic matter constitutes humus, faunal, and microbial biomass dissolved organic matter and carbonized organic matter. It releases the nutrients for plant progress, encourages the structural, biological, and physical health of the soil, and is a buffer against the human elements (Maynard et al. 2007). Soil organic organisms are important for the protection of flora and are sources of the nutrients for the plants. SOC is one of the most significant elements of the soil due to its ability to influence plant development as both a source of energy and a trigger for nutrient accessibility through mineralization (Selige et al. 2006). Soil organic carbon behaves both as a sink and as a source of atmospheric carbon and is the largest vigorous terrestrial carbon reservoir. Thus, pool of soil organic carbon is significant in climate alteration processes by acting as a basis of sinks for atmospheric CO_2.

The amount of soil carbon present in soil can vary according to the landscape types and paddock over the time depending on climate (temperature and rainfall), slope, farming methods, land management, soil nutrition, and soil type (Neigh et al. 2014). Soil organic carbon can be assessed and predicted using different vegetation indices like Brightness Index, Greenness Index, NDVI, SAVI/MSAVI, Wetness Index, and Compound Topographic Index as the parameters for the model with the help of band-rationing algorithm and surveyed data (Gupta et al. 2014; Pandey et al. 2014). The traditional method of acquiring data through field is time consuming and involves huge investment. Geospatial techniques, on the other hand, being cost-effective and having synoptic view, can be utilized for predicting SOC through model building. The present study makes an integrated

use of remote sensing data, laboratory data, geostatistical tools, and field data for predicting SOC in Sariska Tiger Reserve in India (Zheng et al. 2004).

2 Materials and methods

2.1 Study area

Sariska Tiger Reserve is a tiger reserve situated in the Alwar district of Rajasthan, India. The landscape of the tiger reserve contains dry deciduous forests, scrub–thorn arid forests, rocks, grasses, and hilly cliffs (Jain and Sajjad 2016a, b). Vegetation of the study area can be classified in two major types, i.e., tropical dry deciduous forest- and tropical thorn forest-based structural attributes (Jain and Sajjad 2016a, b). In terms of the succession, and concept of continuum of vegetation, the large-scale formations in the area are *Acacia catechu* and *Anogeissu spendula* vegetation types (Jain et al. 2016; Kumar et al. 2015). Dhok (*Anogeissus pendula* Edgew.) is the main species of the tree covering over 90% of the area. It is associated with species like Salar (*Boswellia serrata* Planch.) and *Urjan* (*Linnea corommrndelica* Houtt.) which are small trees, with a short usually crooked bole which grow on rocks and dry area. It extends from the Aravalli hills in Rajputana to Bundelkhand and is important tree, not only as a source of timber and fuel but also for clothing dry tracts. *Khair* (*Acacia catechu* Willd.) and Bamboo (*Dendro calamusstrictus* Roxb.) is small- or medium-sized deciduous tree attaining a height of 12–15 m with light feathery crown, the branch let armed with paired and re-curved spines. The study area was divided into square plots of 0.1 hectare, and a total of 30 soil samples were composed from the whole research area (Fig. 1). Measurement of various parameters like species name, height, diameter at breast height (DBH) for all sampled tropical forest trees above 10 cm DBH was carried out.

2.2 Data used

The study utilized satellite, field, and laboratory data. Base map was prepared using Survey of India (SOI) toposheet (1:50,000). Sentinel-2A Multispectral Instrument (MSI) sensor satellite images were for used for predicting soil carbon. The satellite functions in a sun synchronous orbit with a 10-day repeat cycle. Specific bands like 2, 3, 4, 8, and 11 (Blue, Green, Red, NIR and SWIR respectively) with 10 m spatial resolution were used. Sentinel-2A Multi Spectral Instrument (MSI) contains 13 spectral bands ranging from visible to short-wave infrared (SWIR) wavelengths along a 180° phase orbit with 290-km orbital swath. Measurement of sampled trees was carried out in field, and soil parameters were tested in the laboratory.

2.3 The predictor variables (NDVI, SAVI, and RDVI)

NDVI, RDVI, and SAVI were derived using blue, green, red, and near-infrared bands of the satellite data to assess the biophysical status of surrounding soil (Kumar et al. 2016; Tomar et al. 2013). The NDVI is a modest graphical indicator that can be used to define the greenness, the relative density, and healthiness of vegetation (Powell et al. 2010). This is calculated using Eq. 1. Red band has maximum absorption by the leaf pigments, and infrared band has maximum reflectance due to leaf cellular structure.

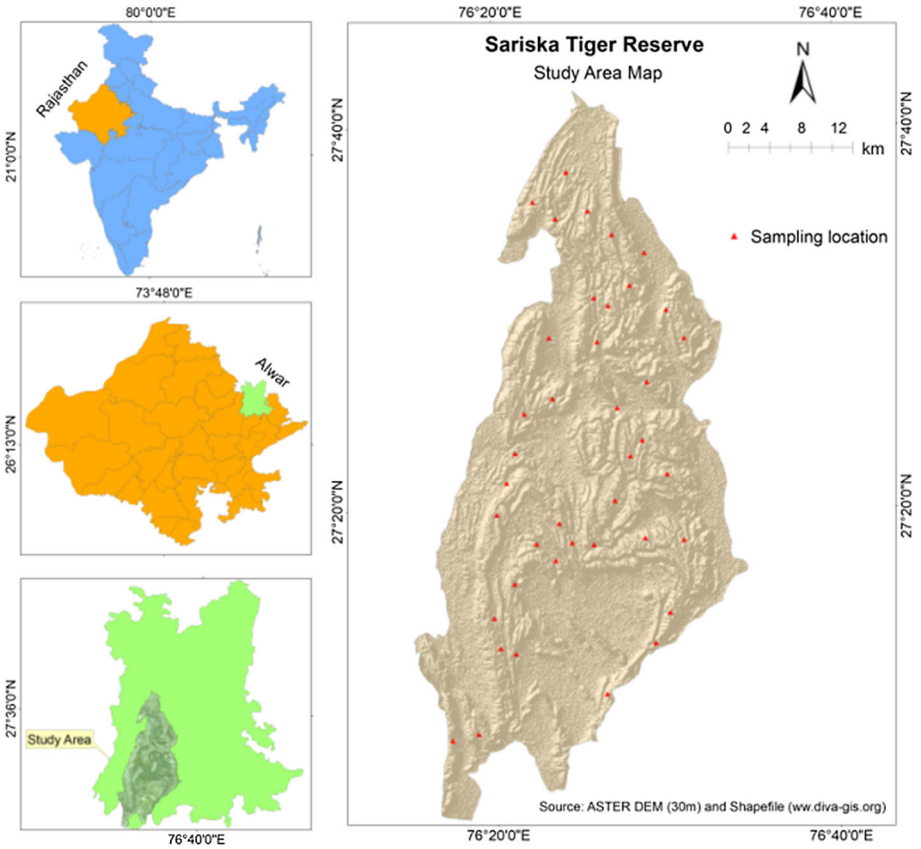

Fig. 1 Location map of study area

$$\mathrm{NDVI} = \frac{R_{\mathrm{NIR}} - R_{\mathrm{RED}}}{R_{\mathrm{NIR}} + R_{\mathrm{RED}}} \tag{1}$$

SAVI or Modified Soil Adjusted Vegetation Index (MSAVI) is approximately similar to NDVI, but MSAVI diminishes the consequence of bare soil on the SAVI (Richardson and Wiegand 1977; Huete 1988). It is calculated by using Eq. 2 (Qi et al. 1994).

$$\mathrm{MSAVI} = \frac{1}{2}\left\{2(R_{\mathrm{NIR}} + 1) - \sqrt{(2 * R_{\mathrm{NIR}} + 1)^2 - 8(R_{\mathrm{NIR}} - R_{\mathrm{RED}})}\right\}. \tag{2}$$

RDVI is generally used to analyze the vegetation at growth stage and the amount of greenness present in the vegetation. RDVI was calculated using the following equation:

$$\mathrm{RDVI} = \frac{(R_{\mathrm{NIR}} - R_{\mathrm{RED}})}{\sqrt{R_{\mathrm{NIR}} + R_{\mathrm{RED}}}} \tag{3}$$

2.4 Soil carbon analysis from field data

Walkey–Black procedure was followed for estimating soil organic carbon at 5 cm depth of soil, where the sampler radius is 3.8 cm and sampler volume is 226.8229 cm^3. Bulk density (g/cm^3) and soil carbon content (%) were calculated from the soil data collected from 30 locations in the study area (Table 1). Bulk density is determined using Eq. (4) (Vagen and Winowiecki 2013; Grossman and Reinsch 2002). We applied drying procedure and baked soil carbon content at 900 °C using an NC-Analyzer Model Sumigraph-NC 90A. Soil carbon and bulk density are calculated by using Eqs. 4 and 5:

Table 1 Summary of field sampling in Sariska Tiger Reserve

Sampling unit	Sampler radius (cm)	Soil depth (cm)	Soil weight (gm)	Bulk density (g/m^3)	Sampler area (m^2)	SOC (g/m^2)	SOC (t/ha)	SOC (%)
1	3.8	5	360	1.58714	0.004536	190.4569	1.9046	0.24
2	3.8	5	320	1.41079	0.004536	1488.3853	14.8839	2.11
3	3.8	5	342	1.50778	0.004536	1085.6042	10.8560	1.44
4	3.8	5	348	1.53424	0.004536	1971.4933	19.7149	2.57
5	3.8	5	347	1.52983	0.004536	872.0016	8.7200	1.14
6	3.8	5	362	1.59596	0.004536	1771.5136	17.7151	2.22
7	3.8	5	322	1.41961	0.004536	631.7261	6.3173	0.89
8	3.8	5	330	1.45488	0.004536	1142.0800	11.4208	1.57
9	3.8	5	306	1.34907	0.004536	829.6778	8.2968	1.23
10	3.8	5	315	1.38875	0.004536	2083.1222	20.8312	3.0
11	3.8	5	300	1.32262	0.004536	1534.2360	15.3424	2.32
12	3.8	5	344	1.51660	0.004536	2654.0520	26.5405	3.5
13	3.8	5	325	1.43284	0.004536	1103.2832	11.0328	1.54
14	3.8	5	356	1.56951	0.004536	776.9054	7.7691	0.99
15	3.8	5	345	1.52101	0.004536	1475.3795	14.7538	1.94
16	3.8	5	364	1.60478	0.004536	946.8176	9.4682	1.18
17	3.8	5	341	1.50337	0.004536	2059.6237	20.5962	2.74
18	3.8	5	308	1.35789	0.004536	1093.0991	10.9310	1.61
19	3.8	5	311	1.37111	0.004536	1295.7020	12.9570	1.89
20	3.8	5	321	1.41520	0.004536	2059.1167	20.5912	2.91
21	3.8	5	335	1.47692	0.004536	2104.6147	21.0461	2.85
22	3.8	5	345	1.52101	0.004536	1505.7997	15.0580	1.98
23	3.8	5	355	1.56510	0.004536	1291.2051	12.9121	1.65
24	3.8	5	356	1.56951	0.004536	1239.9096	12.3991	1.58
25	3.8	5	352	1.55187	0.004536	1365.6464	13.6565	1.76
26	3.8	5	344	1.51660	0.004536	1107.1188	11.0712	1.46
27	3.8	5	305	1.34466	0.004536	826.9664	8.2697	1.23
28	3.8	5	325	1.43284	0.004536	845.3729	8.4537	1.18
29	3.8	5	320	1.41079	0.004536	1403.7378	14.0374	1.99
30	3.8	5	315	1.38875	0.004536	784.6427	7.8464	1.13

$$\text{Bulk density}\left(\text{g/cm}^3\right) = \frac{\text{Mass of oven} - \text{dried soil}}{\text{Total volume}}, \tag{4}$$

$$\text{Soil carbon}(\text{t/ph}) = \text{Soil depth} * \text{soil bulk density} * \text{carbon content}\,(\%\ ). \tag{5}$$

2.5 Assessing relation between SOC and LAI

SOC is found in soil as a constituent of various biochemical multiplexes. Thus, SOC having such biochemical cannot be extracted from the satellite data. In order to delineate SOC through remote sensing, a constraint (terrestrial surface reflectance) has to be linked SOC, which would represent a strong correlation among them. Leaf area index was derived using Landsat 8, and OLI image was used for delineating SOC through spectral characteristic.

$\text{LAI}_{\text{satellite}}$ was calculated in two successive processes. Firstly, the soil fraction (F_{C}) covered by plants was calculated using equation *via* (Choudhury et al. 1994).

$$F_{\text{C}} = \left(\frac{\text{NDVI}_{\max} - \text{NDVI}}{\text{NDVI}_{\max} - \text{NIDVI}_{\min}}\right). \tag{6}$$

Again on 1998, Campbell and Normann stated the soil fraction index using LAI, as mentioned below (Eq. 6). So LAI can be derived by simplifying Eqs. (7) and (8)

$$F_{\text{C}} = \exp\,(-K_{\text{be}}(0) * \text{LAI}), \tag{7}$$

F_{C} = soil fraction covered by plants of given pixel; $K_{\text{be}}(0)$ = spherical leaf angle distribution = 0.5 (standard)

So, leaf area index can be simplified as;

$$\text{LAI}_{\text{satellite}} = -2\text{Ln}(1 - F_{\text{C}}). \tag{8}$$

The spectral linear relationship between LAI and SOC was evaluated through linear regression analysis.

2.6 SOC extraction using Kriging method

Location points of SOC were interpolated using Kriging method (Oliver 1990). This method weights the neighboring dignified values and provides an estimate for an unmeasured plot location. The statistical values for autocorrelation models were calculated through variograms and covariance functions. The model predicts the unknown values after autocorrelation of the data. Prediction value for unmeasured location is calculated by using Eq. 9:

$$Z(s_O) = \sum_{i=1}^{N} \lambda_i Z(S_i) \tag{9}$$

$Z(s_O)$ = prediction value for unmeasured location; $Z(S_i)$ = ith location by measured value; λ_i = ith location by an unidentified weight for the estimated value; N = the number of measured value

2.7 Model validation

Observed (y) and predicted as ($\hat{y}$) values were divided into two groups for each land-cover type (Black 1965). The ground measured SOC was taken as the observed variable and the SOC extracted from satellite data as the predictors. The results were validated by comparing the (root-mean-square error (RMSE) as well as absolute RMSE (Eq. 10).

$$\mathrm{RMSE} = \sqrt{\frac{\left(\check{Y} - Y\right)^2}{N}} \tag{10}$$

3 Result and discussion

3.1 Predictor variable

NDVI (Fig. 2a) for the study area ranges from − 0.41 to + 0.43. Features like barren rock, sand, or snow displayed very low NDVI values (0.1 or less) (Kumar et al. 2014). Scarce vegetation such as bushes and grasslands or crops showed moderate NDVI values (approximately 0.2–0.5). Similarly SAVI (Fig. 2b) is also a kind of vegetation index which is used for enhancing vegetation brightness in low-vegetation canopy areas using background adjustment factor. SAVI values for the study area varied from -0.6 to 0.63. The value beyond 0.2 indicated diminishing of the soil brightness (Kumar et al. 2013; Tomar et al. 2014).

3.2 Analysis of SOC using field data

A summary of the carbon stocks for the whole part of research area is shown in Table 1. The range of SOC stock varies from 1.90 to 26.55 t/ha in the study area. SOC is mostly found in the core zone of tiger reserve area, where as lowest values are found all around the border of the study area.

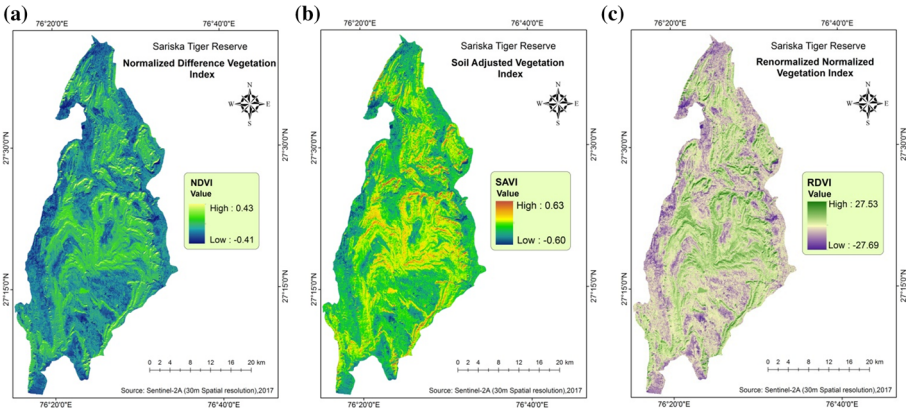

Fig. 2 Mapping of predictor variables using remote sensing data: **a** Normalized Vegetation Index, **b** Soil Adjusted Vegetation Index, **c** Renormalized Vegetation Index

3.3 Analysis of LAI and SOC relationship

The soil fraction value (Fig. 3a) for the study area ranges from − 0.01 to + 1.00. The value beyond + 0.1 is for those soil surfaces which are covered by the plants. LAI (Fig. 3b) varied from − 0.91 to + 0.56 m. Low LAI found in the study area is associated with the texture of sandy soil. The LAI variation was found to be caused by altered management practices. The effect of biophysical factors on LAI was found to be almost identical in the entire study area.

A regression investigation was accomplished between SOC (predicted and field data) and LAI to explore their relationship. We performed regression analysis twice: first between predicted SOC and LAI, and second between LAI and field SOC data. The coefficient of regression (R^2) was resulted to 95% for the first case (Fig. 4a) and 79% for the second case (Fig. 4b). The analysis revealed that significant correlation was found between predicted SOC and LAI, as p value is less than 0.05 (0.032 < 0.005). So LAI can be used as a constraint for extracting SOC using remote sensing.

3.4 SOC prediction

The SOC map generated from Kriging model using Landsat OLI data clearly shows variation in the SOC stocks. The map showed spatially interpolated SOC stocks and helped in assessing the complexity of SOC storage in the Sariska Tiger Reserve. It is observed that the stock decreases with the increasing slope. Among the various categories of land-use/land-cover, vegetation has the maximum content of carbon stock, followed by the

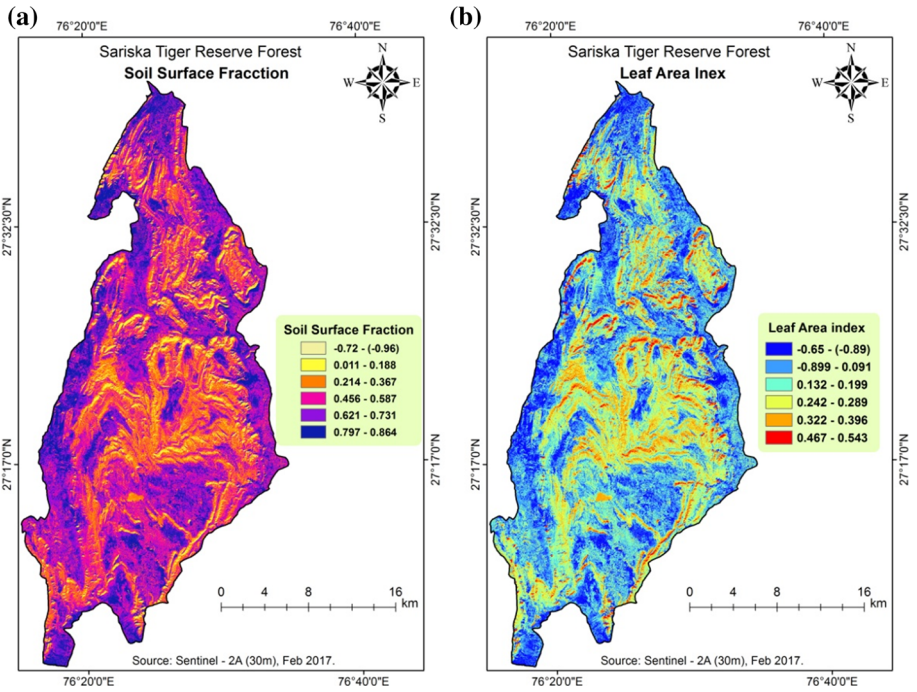

Fig. 3 **a** Soil surface fraction and **b** leaf area index

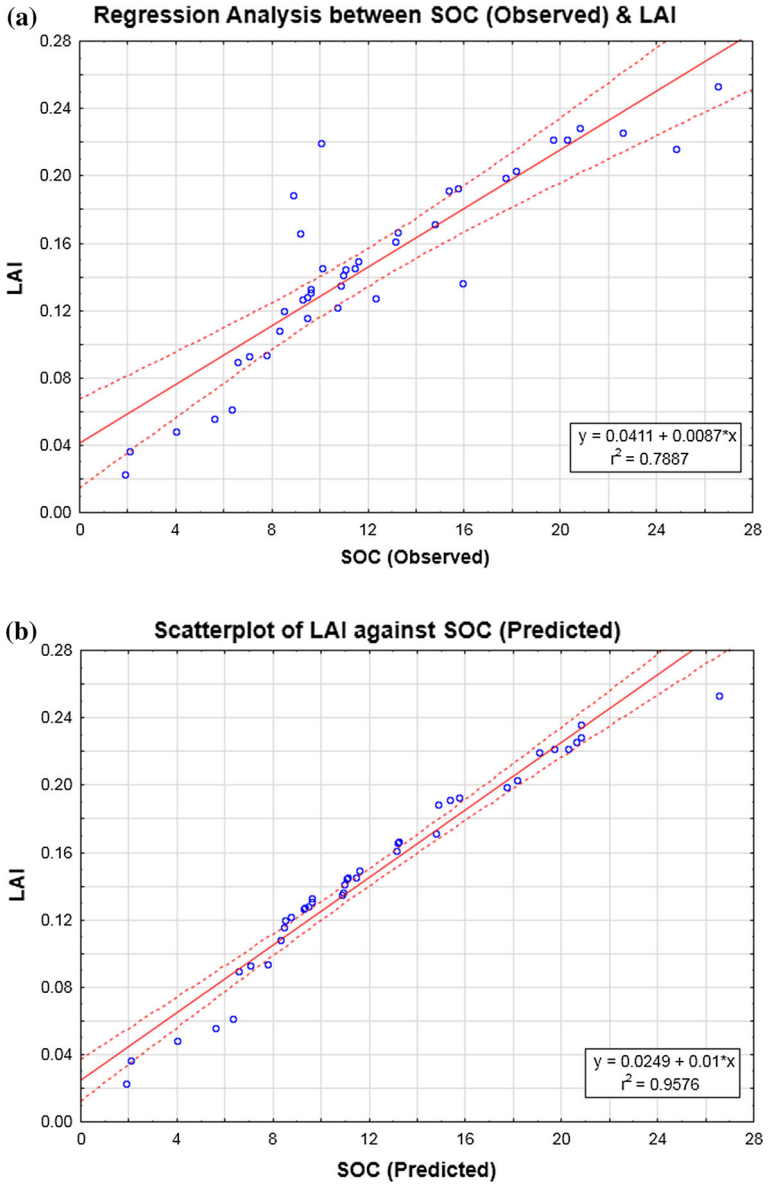

Fig. 4 **a** Regression analysis between SOC (predicted) and LAI. **b** Regression analysis between SOC (observed) and LAI

agricultural, fallow lands, and is very low at the settlement. Vegetation has a higher stock of SOC due to healthy vegetation that gives a steady supply of organic matter to the stock after decomposition. Fallow lands are open lands with little shrub bery, so they have greater stock than settlements. SOC stock and its spatial distribution is shown in Fig. 5. The interpolated the value for the entire study area ranges from 0.273 to 19.064 t/ha.

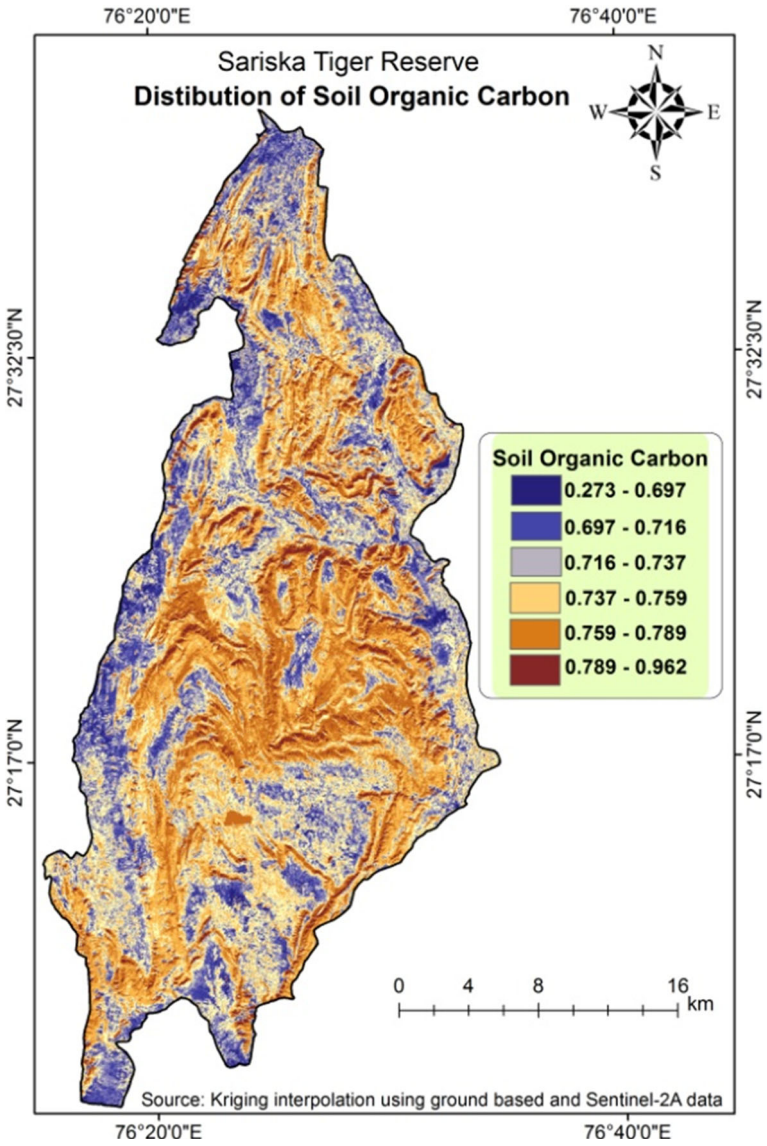

Fig. 5 Predicted soil organic carbon stock at Sariska Tiger Reserve

3.5 Validation of results

The RMSE is calculated using Eq. 10 where in $\check{Y}$ was taken as predicted SOC and Y as observed SOC from the field data. The model accuracy was found to be 0.89. Kriging method has given an acceptable result in this study due to the collection of more number of predictors (sampling) for this model. A positive and strong affiliation was found between the SOC (Predicted from the satellite image) and leaf area index ($LAI_{satellite}$). Regression analysis revealed strong relationship between the leaf area index and predicted SOC.

Spectral reflectance of soil organic carbon with multiplex biochemical cannot be measured precisely and there fore cannot be monitored directly using remote sensing data.

4 Conclusion

The study predicted soil organic carbon distribution using field inventory data in Sariska Tiger Reserve, India. The distribution of carbon stock across the reserve was modeled by Kriging geospatial interpolation technique using Landsat 8 OLI data. We predicted SOC using leaf area index derived through satellite data. LAI can be significantly used as a good constraint for calculating SOC, as the regression for the $LAI_{satellite}$ and SOC (predicted) was found to be $R^2 = 0.95$, with p value less than 0.05. Spatial distribution of SOC shows that forest has maximum stock followed by agricultural lands, while built-up area has the lowest stock. The findings further revealed low SOC concentration along steep slopes. Prediction of soil organic carbon may help in efficient management of forest. Higher-resolution satellite data and Kriging algorithm for soil characteristic can provide accurate information for monitoring health of tree species in different geographical regions at various scales.

References

Barnes EM, Sudduth KA, Hummel JW, Lesch SM, Corwin DL, Yang C, Daughtry CST, Bausch WC (2003) Remote- and ground-based sensor techniques to map soil properties. Photogramm Eng Remote Sens 69(6):619–630

Black CA (1965) Hydrogen-ion Activity. Methods of soil analysis part II: chemical and microbiological properties. America Society of Agronomy, Madison, pp 771–1572

Brown S (1997) Estimating biomass and biomass change of tropical forests. FAO Forest Resources Assessment Publication, Rome, p 55

Campbell GS, Norman JM (1998) An introduction to environmental biophysics. Springer, New York, p 268

Choudhury BJ, Ahmed AH, Idso SB, Reginato RJ, Daughtry CST (1994) Relations between evaporation coefficients and vegetation indices studied by model simulations. Remote Sens Environ 50:1–17

Gao BC, Goetz AFH (1990) Column atmospheric water vapor and vegetation liquid water retrievals from airborne imaging spectrometer data. J Geophys Res 95:3549–3564

Grossman RB, Reinsch TG (2002) The solid phase: 2.1. In: Bulk density and linear extensibility: methods of soil analysis, part 4; Soil Science Society of America Madison, Madison, WI, USA, pp 201–225

Gullison RE, Frumhoff PC, Canadell JG, Field CB, Nepstad DC, Hayhoe K, Avissar R, Curran LM, Friedlingstein P, Jones CD (2007) Tropical forests and climate policy. Science 316:985–986

Gupta G, Singh J, Pandey PC, Tomar V, Rani M, Kumar P (2014) Geospatial strategy for estimation of soil organic carbon in tropical wildlife reserve. In: Srivastava P, Mukherjee S, Gupta M, Islam T (eds) Remote sensing applications in environmental research. Society of earth scientists series. Springer, Cham, pp 69–83

Houghton RA, Hall F, Goetz S (2009) Importance of biomass in the global carbon cycle. J Geophys Res 114:1–13

Huete AR (1988) A soil-adjusted vegetation index (SAVI). Remote Sens Environ 25:295–309

Jain P, Sajjad H (2016a) Analysis of willingness for relocation of the local communities living in the Critical Tiger Habitat of the Sariska Tiger Reserve, India. Local Environ 21(11):1409–1419

Jain P, Sajjad H (2016b) Household dependency on forest resources in the Sariska Tiger Reserve (STR), India: Implications for management. J Sustain For 35(1):60–74

Jain P, Ahmed R, Sajjad H (2016) Assessing and monitoring forest health using a forest fragmentation approach in Sariska Tiger Reserve, India. J Geogr 70(5):306–315

Kumar P, Singh BK, Rani M (2013) An efficient hybrid classification approach for land use/land cover analysis in a semi-desert areausing ETM+ and LISS-III sensor. IEEE Sens J 13(6):2161–2165

Kumar P, Tomar V, Srivastava P, Singh J, Gupta G (2014) Geospatial approach for carbon sink in the timbered biomass for tropical wildlife reserve. Asian J Geoinform 14(1):1–7

Kumar P, Pandey PC, Kumar V, Singh BK, Tomar V, Rani M (2015) Efficient recognition of forest species biodiversity by inventory-based geospatial approach using LISS IV sensor. IEEE Sens J 15(3):1884–1891

Kumar P, Pandey PC, Singh BK, Katiyar S, Mandal VP, Rani M, Tomar V, Patairiya S (2016) Estimation of accumulated soil organic carbon stock in tropical forest using geospatial strategy. Egypt J Remote Sens Space Sci 19(1):109–123

Maynard CL, Lawrence RL, Nielsen GA, Decker G (2007) Modeling vegetation amount using bandwise regression and ecological site descriptions as an alternative to vegetation indices. GISci Remote Sens 44:68–81

McBratney AB, Mendonca Santos ML, Minasny B (2003) On digital soil mapping. Geoderma 117:3–52

Neigh CSR, Bolton DK, Diabate M, Williams JJ, Carvalhais N (2014) An automated approach to map the history of forest disturbance from insect mortality and harvest with Landsat Time-Series data. Remote Sens 6:2782–2808

Oliver MA (1990) Kriging: a method of interpolation for geographical information systems. Int J Geogr Inf Syst 4:313–332

Pandey PC, Tate NJ, Balzter H (2014) Mapping tree species in coastal portugal using statistically segmented principal component analysis and other methods. IEEE Sens J 14(12):4434–4441

Powell SL, Cohen WB, Healey SP, Kennedy RE, Gretchen GM, Pierce KB, Ohmann JL (2010) Quantification of live aboveground forest biomass dynamics with Landsat time-series and field inventory data: a comparison of empirical modeling approaches. Remote Sens Environ 114:053–1068

Qi J, Chehbouni A, Huete AR, Kerr YH, Sorooshian S (1994) A modified soil vegetation adjusted index. Remote Sens Environ 48(2):119–126

Richardson AJ, Wiegand CL (1977) Distinguishing vegetation from soil background information. Photogramm Eng Remote Sens 43:1541–1552

Selige T, Böhner J, Schmidhalter U (2006) High resolution topsoil mapping using hyperspectral image and field data in multivariate regression modelling procedures. Geoderma 136(1–2):235–244

Tekin Y, Tumsavas Z, Mouazen AM (2012) Effect of moisture content on prediction of organic carbon and pH using visible and near-infrared spectroscopy. Soil Sci Soc Am J 76:188–198

Tomar V, Kumar P, Rani M, Gupta G, Singh J (2013) A satellite-based biodiversity dynamics capability in tropical forest. Electron J Geotech Eng 18:1171–1180

Tomar V, Mandal VP, Srivastava P, Patairiya S, Singh K, Ravisankar S, Natesan N, Kumar P (2014) Rice equivalent crop yield assessment using MODIS sensors' based MOD13A1-NDVI data. IEEE Sens J 14(10):3599–3605

Vagen TG, Winowiecki LA (2013) Mapping of soil organic carbon stocks for spatially explicit assessments of climate change mitigation potential. Environ Res Lett 8:1748–1793

Wu CY, Jacobson AR, Laba M, Baveye PC (2009) Alleviating moisture content effects on the visible near-infrared diffuse-reflectance sensing of soils. Soil Sci 174:456–465

Zheng D, Rademacher J, Chen J, Crow T, Bresee M, Le Moine J, Ryu S (2004) Estimating aboveground biomass using Landsat 7 ETM+ data across a managed landscape in Northern Wisconsin, USA. Remote Sens Environ 93:402–411